



DTIC® has determined on 07/16/2010 that this Technical Document has the Distribution Statement checked below. The current distribution for this document can be found in the DTIC® Technical Report Database.

- DISTRIBUTION STATEMENT A.** Approved for public release; distribution is unlimited.
- © COPYRIGHTED;** U.S. Government or Federal Rights License. All other rights and uses except those permitted by copyright law are reserved by the copyright owner.
- DISTRIBUTION STATEMENT B.** Distribution authorized to U.S. Government agencies only (fill in reason) (date of determination). Other requests for this document shall be referred to (insert controlling DoD office)
- DISTRIBUTION STATEMENT C.** Distribution authorized to U.S. Government Agencies and their contractors (fill in reason) (date of determination). Other requests for this document shall be referred to (insert controlling DoD office)
- DISTRIBUTION STATEMENT D.** Distribution authorized to the Department of Defense and U.S. DoD contractors only (fill in reason) (date of determination). Other requests shall be referred to (insert controlling DoD office).
- DISTRIBUTION STATEMENT E.** Distribution authorized to DoD Components only (fill in reason) (date of determination). Other requests shall be referred to (insert controlling DoD office).
- DISTRIBUTION STATEMENT F.** Further dissemination only as directed by (inserting controlling DoD office) (date of determination) or higher DoD authority.
Distribution Statement F is also used when a document does not contain a distribution statement and no distribution statement can be determined.
- DISTRIBUTION STATEMENT X.** Distribution authorized to U.S. Government Agencies and private individuals or enterprises eligible to obtain export-controlled technical data in accordance with DoDD 5230.25; (date of determination). DoD Controlling Office is (insert controlling DoD office).

Photochemical damage from chronic 458-nm laser exposures in an artificially pigmented hTERT-RPE1 cell line

Michael S. Foltz^a, Norris A. Whitlock^{b*}, Larry E. Estlack^c, Manuel A. Figueroa^b, Robert J. Thomas^b, Benjamin A. Rockwell^b, and Michael L. Denton^{a†}

^aNorthrop Grumman, San Antonio, TX 78228-1330;

^bU.S. Air Force AFRL/HEDO[‡], Brooks City-Base, TX 78235-5278;

^cConceptual Mindworks, Inc., San Antonio, TX 78228-1330

ABSTRACT

Artificially pigmented hTERT-RPE1 cells were exposed to a mode-locked or continuous wave (CW) laser at 458 nm for one hour in a modified culture incubator. Exposure conditions were selected to give greatest likelihood of damage due to a photochemical mechanism, with interest in possible differences between CW and mode-locked damage thresholds. After post-exposure-recovery (PER) for either 1-hour or 24-hour, cells were concurrently stained with annexin V and 6-CFDA to determine if they had undergone necrosis or apoptosis. Alternatively, cells were stained with Ethidium Homodimer (EthD-1) and Calcein AM to determine if they had undergone necrosis following 1-hour and 24-hours PER. Preliminary results indicate that laser exposure induced some apoptosis following 1-hour PER, with irradiance required for apoptosis being lower than that for necrosis with mode-locked exposure conditions. Probit analysis yielded necrosis thresholds for cell culture following 1-hour PER using data compiled from both dye sets. CW exposures resulted in a lower threshold than mode-locked exposures for necrosis following 1-hour PER. A thermal model provided the predicted temperature rise in cell culture due to laser exposure. The thermal model validates our choice of laser parameters to obtain photochemical damage. Data following 24-hours PER were inconclusive. Considerations of cell migration are included in the interpretation of data and further improvements to methods when using live cell assays are recommended.

Keywords: photochemical, necrosis, apoptosis, RPE, blue light, cell culture dynamics, modeling

1. INTRODUCTION

The American National Standard for Safe Use of Lasers (ANSI Z136.1-2000) currently states that there is no difference between continuous wave (CW) and mode-locked lasers as pertains to retinal damage thresholds.¹ Thomas *et al.* conducted supplementary research to determine possible differences between CW and mode-locked laser exposure using a primate animal model.² With exposure duration of 0.25 s and a wavelength of 800 nm, this study yielded results in support of this conclusion.² It should be noted that quarter-second exposure durations cause laser damage in the thermal regime, according to information in the literature.^{1,3} We believe that additional research is needed to determine whether conditions appropriate for laser damage in the photochemical regime result in different damage thresholds for CW and femtosecond mode-locked lasers. This difference may exist due to increased effects of two-photon chemical reactions over single-photon reactions. This could result in a lower damage threshold from mode-locked laser exposure when compared to CW laser exposure.

Experiments were conducted using an hTERT-RPE1 cell line, which was artificially pigmented with bovine melanosomes as previously described by Denton *et al.*⁴ Ham *et al.* addressed the need for use of models that contain melanosomes as the primary pigment for observation of chronic blue light damage.³ We chose 458

* Current address: Lexicon Genetics, The Woodlands, TX 77381-1160

† michael.denton.ctr@brooks.af.mil; phone 1 210 536-8396

‡ Opinions, interpretations, conclusions, and recommendations are those of the authors and are not necessarily endorsed by the United States Air Force

nm chronic exposures to allow for experimental testing of the hypothesis that a difference in damage thresholds exists between CW and mode-locked laser exposures, in the regime for photochemical damage. We believe the low average power and photochemical nature of the laser damage mechanism would provide an improved possibility of observing different damage thresholds for CW and mode-locked laser exposure. In addition, our experimental setup included a novel modified incubator design, which allowed for laser exposure to cell culture while temperature was maintained at 37°C (physiologic conditions). The incubator design allowed simultaneous exposure of cells by CW and mode-locked lasers.

Most laser safety work to date has been done using animal models of various types, dependent on the tissue of interest.^{2,3,5-12} Animal models are important and useful, as data from these models incorporate entire tissue samples and immune response. However, experiments using animal models are both expensive and time consuming, particularly for experiments using primates, which are often the model of choice for studies on retinal damage mechanisms.^{2,3, 6-7} We believe that cell culture models can be useful tools to better understand results from animal models and to aide in development of computer models. Use of cell culture models allows for easier determination of specific input parameters for computer modeling: absorbance, reflectance, temperature rise, etc. Also, cell culture is physically simpler to model, as there are fewer components to characterize. Advantages of cell culture include the ability to alter tissue properties, conduct genomics and proteomics, and perform direct measurements of tissue properties and reactions, in addition providing an unlimited supply of tissue for experimentation. We do not believe that cell culture will preclude the use of animals, but it could serve as an additional means for obtaining information about laser damage mechanisms. Additionally, cell culture models may enable reduction in the number of animals used for experimentation in some cases, as the utility of these models is exploited.

Within the scope of this paper, we establish a method for consistently obtaining necrosis endpoints (ethidium/calcein) following 1-hour laser exposure and 1-hour post-exposure-recovery (PER), in a modified incubator setup. A possible method for detection of early onset apoptosis (annexin/CFDA) was investigated for use with our cell model. Results indicate that a difference in necrosis threshold may exist between CW and mode-locked laser exposure following 1-hour PER, with CW being more damaging than mode-locked. This indicates that mode-locked laser exposures were insufficient to result in significant contribution to two-photon over single-photon effects. Following 1-hour PER, an unexpected result of early onset apoptosis was observed. Possible cell "fill-in" or replacement into the laser exposure region was observed following 24-hours PER. This suggests that 24-hours PER may be excessive for observation of delayed effects in our cell model. We recommend PER between 1-hour and 24-hours for observation of delayed effects, to avoid complications arising from cell replacement.

2. MATERIALS AND METHODS

2.1 Cell Culture

All cell culture media were obtained through CellGro, with the exception of Fetal Bovine Serum (Atlanta Biologicals, S11150) and HEPES (Fisher Scientific, BP299-100). The cell culture model used in this experiment consisted of an hTERT-RPE1 cell line, passed in T-75 cell culture flasks (Corning, 430641), with 1:10 split at 3-4 day intervals. Cells were maintained at 37°C with 5% CO₂ during growth and plating prior to laser exposures. At split, cells were plated in 48-well cell culture plates (Corning, 3548) at 70,000 cells per well in 300 µl Growth Media (GM). GM consists of DMEM/F12 (15-090-CM) supplemented with 10% Fetal Bovine Serum, 100 I.U./ml Penicillin and 100 µg/ml Streptomycin (3000-2CI), 1 mM L-Glutamine (2500-5CI), 50 µg/ml Gentamycin (30-005-CR), and 10 mM HEPES. Exposure media (EM) for this experiment was DMEM (without phenol red) supplemented with 2% bovine serum albumin (Fisher Scientific, BSA Fraction V), 100 I.U./ml Penicillin and 100 µg/ml Streptomycin, 1 mM L-Glutamine, 50 µg/ml Gentamycin, and 10 mM HEPES. Hanks Balanced Salt Solution or HBSS (21-021-CM) was utilized for washes, unless otherwise noted. One day following plating, 10 µl bovine melanosome stock were added to the cells, as described in a work by Denton *et al.*⁴ On the first or second day following melanosome addition, cell culture was washed twice in EM and exposed to lasers for 1-hour in 100 µl EM. Cells were then allowed to recover for 1 or 24 hours in 300 µl fresh GM in a 37°C incubator with 5% CO₂ prior to staining.

2.2 Dye Information

Annexin V-Cy3.18 and 6-CFDA (Sigma Aldrich, APOAC-1KT) combination stain was used for one portion of this experiment. Stock solutions were initially prepared for Annexin and 6-CFDA at concentrations of 100 $\mu\text{g}/\text{ml}$ in DMSO and 50 mM in acetone, respectively. On exposure days, stock solutions were then diluted to working concentrations in phosphate buffered saline (PBS) to 1 $\mu\text{g}/\text{ml}$ Annexin and 125 μM 6-CFDA. The staining procedure involved washing cells twice with ice cold PBS, washing three times with 1x binding buffer, and addition of 100 μl dual dye preparation at working concentrations. The cells were then incubated at room temperature with the dye for 15 minutes. The dye was then removed and the cells were washed four times with binding buffer. Binding buffer was left over the cells (200 μl) for imaging at the microscope. The LIVE/DEAD Viability/Cytotoxicity kit (Molecular Probes, L-3224), which contains Ethidium Homodimer (EthD-1) and Calcein AM, was used for another portion of this experiment. Stocks solutions were initially prepared for EthD-1 and Calcein AM at concentrations of 2 mM and 4 mM, respectively. These stock solutions were then diluted 1/1000 in HBSS to obtain working solutions on experiment days. The staining procedure involved washing with HBSS and incubating cells with 100 μl working solution for 10 minutes in a 37°C incubator. Dye was then removed, cells were washed, and 300 μl HBSS was placed over cells for imaging. Additional literature on use and interpretation of results from these dye sets is available through Molecular Probes.

2.3 Damage Determination

Cells were visualized using bright field, phase contrast, and fluorescence microscopy with an inverted phase-contrast microscope enabled for fluorescence (Olympus CK-40F). A blue filter cube (Olympus, U-M1002) was used to excite fluorescence in Calcein AM and 6-CFDA. The blue cube consisted of a 475/30 nm bandpass exciter, 510/40 nm bandpass emitter, and 500 nm longpass dichroic. Fluorescence from EthD-1 and annexin was observed using a green filter cube (Chroma, 41007A). The green cube consisted of a 530/30 nm bandpass exciter, a 610/75 nm bandpass emitter, and a 570 nm longpass filter. Images were obtained using a CCD camera (ORCA-100-ER, Hamamatsu). Images were then enhanced with color and overlays were created when necessary using an image acquisition and analysis package (Simple PCI, Compix Inc). Annexin/6-CFDA stain was used for determination of apoptosis/necrosis onset. EthD-1/Calcein was used for necrosis determination only. All images were reviewed by three viewers and scored independently. Agreement between at least 2 viewers was required for determination of endpoints.

2.4 Laser Exposure Setup with Incubated Chamber

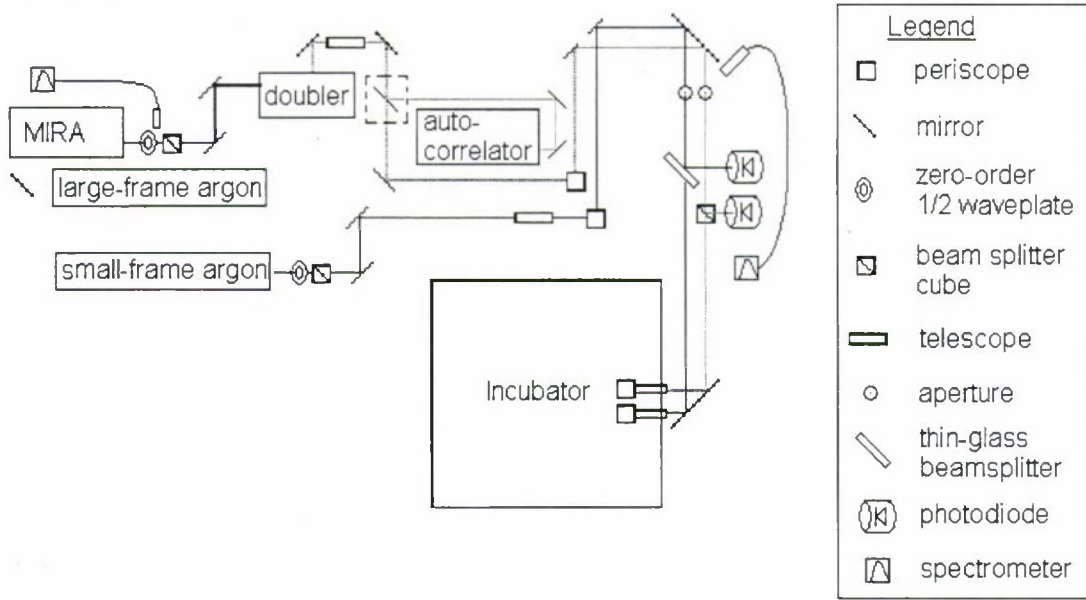
Two lasers were used in this experiment. The output from a Ti:sapphire laser (Coherent, MIRA 900), directed through a second harmonic generation (SHG) crystal (Coherent, Model 4500), generated a mode-locked 457.9-nm beam with 115-fs pulse duration and 76-MHz repetition rate. The pulse duration of the second harmonic was measured using an autocorrelator (APE, Pulse Check) located immediately after the telescope (Figure 1). The CW source was an argon ion laser, which was tuned to 457.9 nm for the duration of the experiment. Two argon ion lasers were used during this experiment (Spectra Physics, model 168B-06 and Lexel, model 85).

A single-lens imaging system was used to create a beam with a 600- μm spot diameter (approximate) at the laser exposure site inside the incubator. The incubator was incorporated into the experimental setup such that cell culture could be maintained under controlled physiologic conditions during laser exposures. Both beams were telescoped to a larger size and then imaged at an aperture to generate quasi-flattop beam profiles. A 400-mm focal length lens was used to image the quasi-flattop beams from the aperture to the sample, with a magnification of 0.1x at the sample. Focus and centering of the imaging system and flattop profile of the beam were checked using a beam profiler (Quantum Composers, Vision 1024). Lasers exposures were centered using burn paper placed in the well bottom of the 48-well plates. Well-plates were secured using metal mounting brackets that allowed the plates to slide from left to right, but restricted movement in the other axis.

The laser output power was adjusted using a half-wave plate/glan prism combination. Laser wavelength was confirmed by a spectrometer. Power was measured at the sample both before and after the experiment using

a power meter (Newport, Model 1830-C) and calibrated silicon detector (Newport, Model 818-SL). Real-time power measures were made during the course of the experiment. This was accomplished by using beam splitters to send a small percentage of each beam to silicon photodiodes prior to the incubator. Power measurements taken before and after laser exposures provided a means for calibrating the real-time measurements from the photodiodes for overall power determination during the course of the experiment.

Figure 1. Laser setup with incubated chamber is shown, which allowed for regulation of physiologic conditions during laser exposure



3. RESULTS

3.1 Damage Endpoints

Analysis of the annexin/6-CFDA dual stain gave three endpoints for exposed cells: viable, apoptotic, and necrotic. Also, EthD-1/calcein dual stain gave two endpoints for exposed cells: viable and necrotic. Examples of cells stained with EthD-1/Calcein AM (necrotic) and Annexin/CFDA (necrotic and apoptotic) following 1-hour PER are shown in Figure 2.

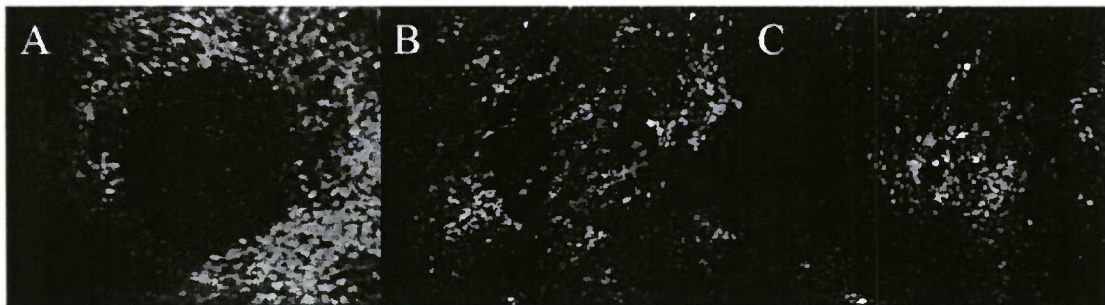


Figure 2. Following 1-hour laser exposure and 1-hour PER, cells were stained with EthD-1/Calcein AM to observe necrosis (A) or with Annexin/CFDA to observe necrosis (B) or apoptosis (C)

Cells exposed to a laser and then stained with EthD-1/Calcein following 1-hour PER appear to show a small difference in lowest irradiance for observation of necrosis: 0.226mW/cm^2 and 0.261mW/cm^2 for CW and mode-locked, respectively (Table 1). This is interesting as it suggests that there is little difference between CW and mode-locked laser exposure for the laser parameters in our experiment, with CW laser exposure

causing laser damage slightly more consistently at lower irradiances. Cells stained with Annexin/6-CFDA were scored for apoptosis and necrosis (Table 1). These data show that cells stained positive for necrosis following exposure to lower irradiances for CW exposure (0.194 W/cm²) than for mode-locked (0.265 W/cm²). In addition, cells stained apoptotic at lower irradiances for CW exposure (0.190 W/cm²) than for mode-locked exposure (0.237 W/cm²). This suggests a difference between CW and mode-locked exposure for both apoptosis and necrosis thresholds following 1-hour PER, with cells being more easily damaged by CW laser exposure. When data are compared between dye sets (annexin/6-CFDA, EthD-1/Calcein) with mode-locked laser exposure, there appears to be little difference between lowest irradiance for observation of necrosis following 1-hour PER: 261mW/cm² and 265mW/cm² for Annexin/1-CFDA and EthD-1/Calcein, respectively (Table 1). However, there appears to be a difference in the lowest irradiance for observation of a necrosis for CW exposure between the two dye sets, with greater sensitivity to necrosis observed using annexin/6-CFDA (0.194 W/cm²) than EthD-1/calcein (0.226 W/cm²). This information suggests that data from EthD-1/calcein and annexin/6-CFDA dye sets can be combined without hesitation for probit analysis of cells following mode-locked exposure, but that similar analysis of data from CW exposed cells may not be appropriate. Additional data should be collected before stronger statements can be made.

Table 1. Endpoints (YES/NO) provided for damage determination following one-hour exposure and one-hour PER.

EthD-1 / Calcein				Annexin / 6-CFDA					
CW		mode-locked		CW			Mode-locked		
Irradiance (W/cm ²)	Necrosis	Irradiance (W/cm ²)	Necrosis	Irradiance (W/cm ²)	Necrosis	Apoptosis	Irradiance (W/cm ²)	Necrosis	Apoptosis
0.097	NO	0.101	NO						
0.101	NO	0.103	NO						
0.116	NO	0.109	NO						
0.124	NO	0.112	NO	0.190	NO	YES	0.187	NO	NO
0.226	YES	0.211	NO	0.194	YES	NO	0.197	NO	NO
0.228	NO	0.212	NO	0.196	YES	NO	0.200	NO	NO
0.251	NO	0.238	NO	0.200	NO	NO	0.201	NO	NO
0.268	YES	0.261	YES	0.202	NO	NO			
0.271	YES	0.269	NO	0.234	YES	NO	0.237	NO	NO
0.273	YES	0.273	YES	0.235	YES	NO	0.237	NO	YES
0.274	YES	0.275	NO	0.238	YES	NO	0.243	NO	NO
0.279	YES	0.277	YES	0.244	YES	NO	0.244	NO	NO
0.284	YES	0.277	YES	0.244	YES	NO	0.247	NO	YES
0.291	YES	0.279	YES	0.251	YES	NO	0.255	NO	YES
0.291	YES	0.298	YES	0.265	NO	NO	0.256	NO	YES
0.300	YES	0.300	YES	0.271	YES	NO	0.265	YES	NO
0.300	YES	0.301	YES	0.277	YES	NO	0.272	NO	YES
0.301	YES	0.303	YES	0.277	YES	NO	0.278	YES	NO
0.301	YES	0.307	YES	0.278	YES	NO	0.284	YES	NO
0.307	YES			0.280	YES	NO	0.285	YES	NO
0.307	YES	0.319	YES						
0.463	YES	0.463	YES						
0.463	YES	0.463	YES						
0.514	YES	0.547	YES	0.656	YES	NO	0.635	YES	NO
5.038	YES	3.913	YES						
5.038	YES	3.913	YES						

Due to insufficient range of data collected, Probit analysis¹³⁻¹⁴ to determine ED₅₀ values with fiducial limits could not be used on data from individual dye sets (EthD-1/Calcein AM, Annexin/6-CFDA). However, data compiled from both dye sets gave ED₅₀ values with good fiducial limits for necrosis following 1-hour PER. The rationale for combining data from these two dye sets is that the endpoint measured was the same (necrosis onset following 1-hour PER) and one dye constituent from each set (Calcein AM/6-CFDA) functioned in similar fashion. Differences observed in Table 2 between CW and mode-locked necrosis thresholds include lower threshold, wider fiducial limits (LFL and UFL), and lower slope and probability of chi-square for CW necrosis threshold. The lower slope and probability of chi-square indicate that the distribution of cross-over values between viable and necrotic is wider for CW data. The wider fiducial limits for CW, particularly the lower fiducial limit, indicate that additional data are needed at lower irradiances. For these reasons, the reported CW necrosis threshold should be observed with caution until enough data can be collected to assure that thresholds from EthD-1/Calcein AM and annexin/6-CFDA do not differ significantly.

	CW	Mode-locked
ED ₅₀ (W/cm ²)	0.207	0.267
UFL (W/cm ²)	0.231	0.276
LFL (W/cm ²)	0.139	0.251
Slope	12.7	59.5
Prob Chi-Sq	0.88	1.00

Table 2. ED₅₀ values were determined by probit analysis of combined necrosis data from Table 1.

3.2 Cell Dynamics Following Laser Exposure

Laser exposed cells were stained with EthD-1/Calcein AM following 1-hour and 24-hours PER and imaged as described in the methods. One example of high (Figure 3) and low (Figure 4) irradiance exposures are shown for both CW and mode-locked laser exposure. These images are provided to introduce a cell monolayer "fill-in" or replacement theory.

In Figure 3, cell culture was exposed to approximately twenty times the minimum irradiance required for necrosis following 1-hour PER. At 1-hour PER, cells were not able to replace dead cells in the exposure site. Additionally, the boundary for cell death is clearly defined and a small increase in Calcein fluorescence is seen in cells along the boundary. At 24-hours PER, partial replacement of dead cells was observed at the exposure site, resulting in a less clearly defined boundary for cell death. Also, cells along and within the boundary for necrosis appear elongated with a marked increase in Calcein fluorescence. This experiment was repeated with n = 2 to confirm consistency of results.

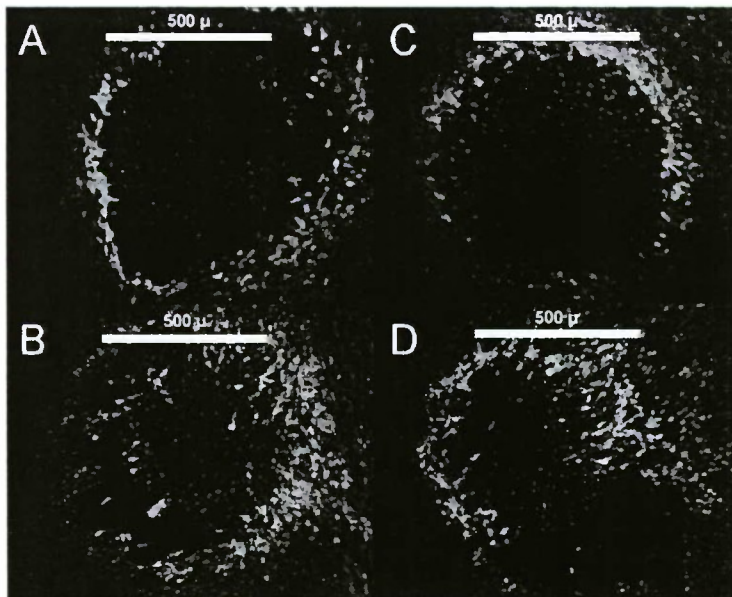


Figure 3. All cells were exposed for 1 hour at an irradiance of approximately 5 W/cm² (CW) or 4 W/cm² (mode-locked). Cells were then stained with EthD-1/Calcein AM as described in methods.

A) CW exposure with 1-hour PER. B) CW exposure with 24-hours PER. C) Mode-locked exposure with 1-hour PER. D) Mode-locked exposure with 24-hours PER.

In Figure 4, cells exposed to approximately two times the minimum irradiance for necrosis following 1-hour PER appear to have a defined region of damage following 1-hour PER. Also, cells along the boundary of the exposure site demonstrate increased Calcein fluorescence. Replacement appears to occur following 24-hours PER. Replacement is particularly noticeable for the mode-locked case following 24-hours PER. Necrotic cells from the laser exposure can still be seen stained positive for EthD-1 beneath the new layer of healthy cells in both CW and mode-locked cases. For CW exposure following 24-hours PER, a defined region with negative Calcein AM is observed, though it is a smaller region than the laser exposure which stained positive for EthD-1. Cells within and along the exposure site following 24-hour PER appear elongated with increased Calcein fluorescence. This experiment was repeated with $n = 3$ to confirm consistency of results.

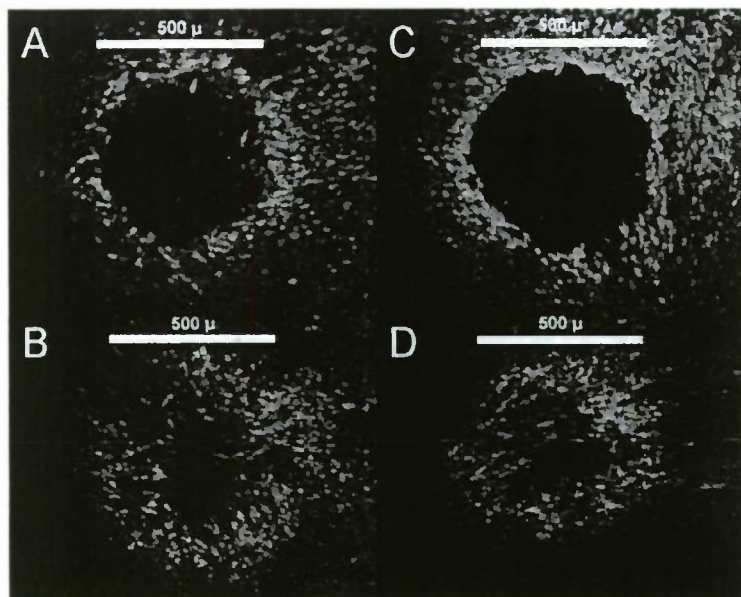


Figure 4. All cells were exposed for 1 hour at an irradiance of approximately $500\text{mW}/\text{cm}^2$. Cells were stained with EthD-1/Calcein AM as described in methods.

A) CW exposure with 1-hour PER. B) CW exposure with 24-hours PER. C) Mode-locked exposure with 1-hour PER. D) Mode-locked exposure with 24-hours PER.

3.3 Bulk Absorption Coefficient Measurement

The bulk absorption coefficient was calculated for the cell samples. Unfortunately, we depleted our supply of melanosome particle (MP) stock from this experiment (old MP stock) before we were able to conduct our absorption measurements. Fortunately, we had already conducted MP counts prior to running out of the old MP stock. A new batch of MP (new MP stock) was used to determine absorption properties of our artificially pigmented cell-line. We utilized a plate reader (Tecan, GENios) to conduct absorbance measurements. Absorbance of cell samples at 460 ± 5 nm, one day after addition various volumes of MP stock, was determined by subtracting the absorbance of the plate with media from the absorbance of the plate, media, cells, and MP. This calculation is believed to account for most losses, such as reflection and absorption due to plate and media. We did not account for scattering or reflection at the surface of the pigmented cells. Measurements were conducted with $n = 7$. The absorbance was used to compute the absorption coefficient via the following formula:

$$\mu_{\text{abs}} = -(\ln(10^{-\text{abs}})/\text{th}_{\text{sample}})$$

Where μ_{abs} is the bulk absorption coefficient, abs is the absorbance at 460 ± 5 nm, and $\text{th}_{\text{sample}}$ is the thickness of the sample. The thickness of the sample was an assumed to be 7 ± 1.5 microns based on depth of focus with laser scanning confocal microscope. Using this information, we computed the absorption coefficient for cells with various volumes of new MP stock added. This allowed us to generate a standard curve for absorption coefficient with respect to MP/well of new MP stock (Figure 5). MP concentration for the batch used in this experiment was determined to be 2.94×10^9 MP/ml at $10\mu\text{l}$ per well, resulting in 2.94×10^7

MP/well. We then compute the absorption coefficient of pigmented cells for this experiment (old MP stock) by extrapolating from the standard curve: $670 \pm 39 \text{ cm}^{-1}$.

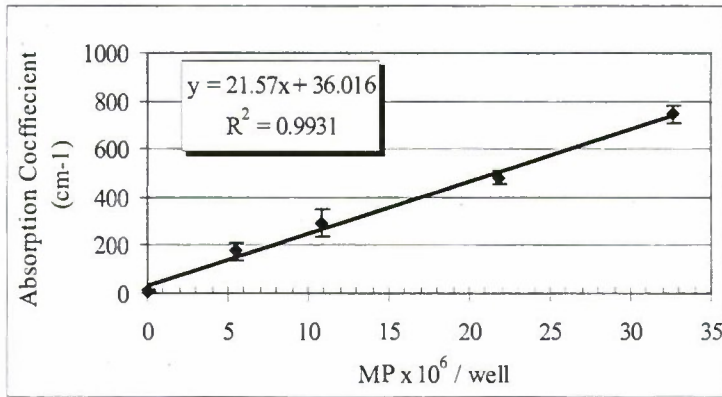


Figure 5. Standard curve for absorption coefficient with respect to concentration MP/well using new MP stock.

3.4 BTE Thermal Model

The "BTE Thermal Model" provided supporting analysis of experimental results.¹⁵⁻¹⁶ The model consists of a numerical solution to the bio-heat equation with source terms appropriate for linear absorption of laser energy by a multi-layer medium.¹⁷⁻¹⁸ The model considers three layers: exposure medium, cell monolayer, and plastic well plate. All layers were assumed to be homogeneous absorbers of uniform thickness. All thermal properties, other than those listed in Table 2, were obtained from sources in the literature. The cell monolayer and exposure medium were assumed to be equivalent to water for the properties of specific heat, thermal conductivity, and density, with values of $4.1868 \text{ J/g/}^\circ\text{C}$, $6.28 \times 10^{-3} \text{ W/cm/}^\circ\text{C}$, and 1 g/cm^3 , respectively.¹⁷ The cell culture microtiter dishes consisted of virgin polystyrene. Estimates of specific heat, thermal conductivity, and density were obtained from www.goodfellow.com, with values of $1.20 \text{ J/g/}^\circ\text{C}$, $1.30 \times 10^{-3} \text{ W/cm/}^\circ\text{C}$, and 1.05 g/cm^3 , respectively. Damage thresholds were determined using a single-term rate process model.¹⁹ Polhamus and Welch's rate process model coefficients for retinal tissue¹⁷, $E = 6.28 \times 10^5 \text{ J/mole}$ and $A = 3.1 \times 10^{99} \text{ s}^{-1}$, were used because they provided the most conservative estimates of thermal retinal damage. Table 2 lists other important input and output parameters for the thermal model.

Input Parameters	Laser*	Spot Diameter (cm)	Irradiance (W/cm^2)
		0.060	0.250
	Cell Monolayer	Thickness (cm)	Absorption Coefficient ($1/\text{cm}$)
	Exposure Medium	0.0007	670
	Well Plate	0.0100	N/A
		0.1390	N/A
Output Parameters	Cell Monolayer	Computed Temperature Rise ($^\circ\text{C}$)	Computed Damage Threshold (W/cm^2)
		0.980	2.864

Table 2. BTE thermal model input parameters and computed output parameters are listed.

* Model assumed use of a CW laser source.

4. DISCUSSION

4.1 Damage Endpoints

The dye set used for necrosis is fairly straightforward, as necrosis is observed for all cells once the damage threshold is exceeded. Additionally, necrosis landmarks are relatively easy to label and observe. This is because most indicators of necrotic damage are immediate and lasting, such as lack of metabolic activity, loss of intact membranes, and marked changes in appearance when observed using phase contrast

microscopy. Apoptosis appears to be much more difficult to characterize. This is partially due to the transient nature of apoptotic events: cells undergo apoptosis at different rates and threshold conditions with dependence on the mode of injury. According to Saraste *et al.*²⁰, "few cells undergoing apoptosis are present at a single time point." Also, Zurgile *et al.*²¹ state that "Since high variability exists within cell populations in regard to the kinetics of the death course, the ability to continuously monitor several apoptotic parameters occurring in single or subgroups of cells may significantly contribute to the identification of apoptotic cells." For this reason, most conclusive papers discussing apoptosis use non-adherent cell models and/or characterize apoptosis over a time course using flow cytometry or video microscopy under physiologic conditions.²⁰⁻²¹ Even in these cases, where cells are chemically treated to obtain synchronized apoptotic events, there is variability over the time course for observation of apoptosis. While flow cytometry is an appealing technique because of the ease with which time course analysis can be conducted on events such as apoptosis, it is impractical and difficult to use such techniques for adherent cell models.²² Other methods for detecting apoptosis include single gel electrophoresis (comet), TdT-dUTP terminal nick end labeling (TUNEL), among others.²³⁻²⁴

Due to the difficulties in measuring apoptosis in adherent cells, we attempted to characterize the apoptosis threshold by observation of a pattern of annexin staining in cells following 1-hour and 24-hours PER. The data for cells following 24-hours PER are not presented in this paper, due to issues with cell replacement. For a laser exposure site to be deemed apoptotic, cells in the laser exposure site needed to stain positive for annexin with little to no loss of CFDA staining. We believe that this is an indication of early onset apoptosis. At 1-hour PER, some apoptosis staining was observed, with staining being more reliable and distinct for mode-locked laser exposures. Apoptosis occurred at slightly lower irradiance than required for necrosis. This observation of apoptosis following 1-hour PER is unexpected, but is consistent with data collected by other researchers as regards observation of early onset apoptosis.²¹⁻²² However, the transient nature of apoptosis threshold determination necessitates consensus between numerous detection techniques. Results are preliminary and require further research, as the time course for apoptosis in our cell model due to laser injury has not yet been determined and threshold determination for apoptosis was somewhat qualitative (i.e. based on visual observation of fluorescence microscopy, with no cell counting). Our results represent a critical first effort to define apoptotic laser damage in our cell culture model for future efforts.

We originally exposed cells to mode-locked and CW laser sources to assess possible differences in necrosis threshold between laser sources capable of generating two-photon chemical reactions (mode-locked) versus those capable only of single-photon reactions (CW). Necrosis was counted if cells were predominately necrotic throughout the laser exposure area. A statistically significant difference was found between CW and mode-locked laser irradiance thresholds of cells following 1-hour PER and observed for necrosis using combined data from both dye sets, with CW threshold being lower than mode-locked. This difference is interesting, but it runs contrary to the expectation of decreased threshold for mode-locked exposure due to the increased contribution of the mode-locked laser to 2-photon chemical reactions. When analyzed as an individual data set, cells stained with EthD-1/Calcein AM following 1-hour PER show no apparent differences between CW and mode-locked exposure. Differences in the compiled data appear to be inferred predominately by inclusion of cells scored for necrosis following 1-hour PER and Annexin/6-CFDA staining. Therefore, caution should be used in interpretation of compiled data from both dye sets until additional data can be collected to determine whether differences exist for threshold determination between the dye sets, specifically for CW exposure. Since results indicate that the mode-locked threshold is either greater or equivalent to the CW threshold following 1-hour PER for necrosis, we conclude that the repetition rate and pulse duration of the mode-locked laser were not optimal for 2-photon chemical reactions. Currently, we are conducting experiments to better define the necrosis threshold following 1-hour exposure and 1-hour PER comparing CW and mode-locked laser exposure, with all data collected using one dye set (EthD-1/Calcein AM).²⁵

4.2 Cell Dynamics Following Laser Exposure

An issue that must be addressed in our cell model is cell replacement following laser exposure, with emphasis on 24-hours PER. Under normal cell culture conditions, our cell culture model has a doubling time of approximately 29 hours. Additionally, the hTERT-RPE1 product reference (Clonetech, 1999) shows that

cell growth is dependent on cell proximity: confluent cultures demonstrate contact inhibition. When laser exposure results in necrosis or apoptosis, the possibility of cell replacement is increased due to reduced contact inhibition from viable cells. We originally did not believe that replacement could occur following 24-hours PER, due simply to the small number of cells boarding the exposure site and the large area of the exposure site (laser diameter of approximately 600 μm). Images taken of cells exposed to approximately 2 and 20 times the necrosis threshold followed by 1-hour and 24-hours PER (Figure 3, Figure 4) give evidence that cell replacement is occurring in our cell system. Following 24-hours PER, the elongated shape of cells in and around the exposure site following laser exposure is indicative of cell migration. Also, an increase in Calcein fluorescence following 1-hour and 24-hours PER, suggests an increase in esterase activity for cells in and around the exposure site, indicating increased metabolic activity. It should be noted that cells outside of the exposure sites do not show these characteristics. Following exposure to 2x necrosis threshold with 24-hours PER, there appears nearly complete recovery in the exposure site. A small difference was observed between CW and mode-locked exposure, with replacement being improved following mode-locked exposure. Observations suggest that replacement (not recovery) is occurring in our cell model. This should be of considerable concern to researchers studying laser-exposed cells *in-vitro*.

4.3 Thermal Model

The BTE thermal model predicts that 1-hour, 460-nm CW laser exposure at an irradiance of 250 W/cm^2 results in a maximum temperature rise of 0.98 $^\circ\text{C}$. Additionally, a required temperature and irradiance threshold for an observed damage radius of 150 μm was computed using the BTE thermal model, with values of 9.0 $^\circ\text{C}$ and 2.864 W/cm^2 , respectively. These predictions suggest that thermal damage is highly unlikely, due to insufficient temperature rise in the RPE monolayer. According to the BTE thermal model, temperature rise and irradiance must be approximately 9 or 11.5 fold greater than the reported necrosis threshold following 1-hour PER for observation of damage due to a thermal mechanism. Therefore, cell death must be due to a non-thermal mechanism, perhaps with minor thermal contribution. The negligible temperature rise predicted by the BTE thermal model is consistent with the conclusion that chronic 458-nm laser light results in photochemical damage. These data are consistent with actual and modeled temperature rises determined using primate retinal models.^{3,6,7} We suggest collection of time-temperature histories to determine how accurately this model approximates temperature rises due to laser exposure. We could then use information collected from our cell culture model to aide in refining the BTE-thermal model to achieve better temperature rise approximations. It should be noted that the BTE thermal model is not expected to provide accurate damage predictions unless a photochemical damage mechanism is incorporated. An understanding of the mechanisms behind laser damage in our cell model may aid in developing a method for incorporation of photochemical damage into the BTE thermal model.

5. CONCLUSIONS

We recommend further research on necrosis and apoptosis in this cell model using a range of PER shorter than 24-hours. Additional experiments should be conducted to follow dynamic changes in laser exposed cells over a PER time course. A method for automated analysis of cells after staining with fluorescent dyes may be useful. Continuation of these experiments would facilitate better understanding of the processes for induction of necrosis and apoptosis in this cell model. A better understanding of tissue response to laser exposure is essential for improving our ability to predict damage and determine methods for protection.

6. REFERENCES

1. ANSI. *Safe Use of Lasers*. Orlando, FL: American National Standards Institute; 2000:Z-136.1-2000.
2. Thomas, R.J., Noogin, G.D., Stolarski, D.J. "A comparative study of retinal effects from continuous wave and femtosecond mode-locked lasers." *Lasers in Surgery and Medicine*. 31:9-17; 2002.
3. Ham, W.T. Jr., Mueller, H.A. "The Pathology and Nature of the Blue Light and Near-UV Retinal Lesions Produced by Lasers and Other Optical Sources" *Laser Applications in Medicine and Biology*. Chapter 5. Plenum Publishing Corporation, 1989.
4. Denton, M.L., Eikum, D.M., Noojin, G.D., Stolarski, D.J., Thomas, R.J., Glickman, R.D., and Rockwell, B.A. "Pigmentation in NIR Laser Tissue Damage," *Proceeding of SPIE*. 4953:78-84, 2003.
5. Cai, J., Nelson, K.C., Wu, M., Sternberg, P. Jr., Jones, D.P. "Oxidative damage and protection of the RPE" *Progress in Retinal and Eye Research*. 19(2):205-21, 2000.
6. Ham, W.T. Jr., Ruffolo, J.J. Jr., Mueller, H.A., Clarke, A.M., Moon, M.E. "Histological analysis of photochemical lesions produced in rhesus retina by short-wave-length light" *Investigative Ophthalmology and Visual Science*. 17(10):1029-1035, 1978.
7. Ham, W.T. Jr., Mueller, H.A., Ruffolo, J.J. Jr., Clarke, A.M. "Sensitivity of the Retina to Radiation Damage as a Function of Wavelength" *Photochemistry and Photobiology*. 29:735-743, 1979.
8. Lin, C.P., Kelly, M.W., Sibayan, S.A.B., Latina, M.A., and Anderson, R.R., "Selective Cell Killing by Microparticle Absorption of Pulsed Laser Radiation." *IEEE Journal of Selected Topics in Quantum Electronics*. 5(4): 963-968, 1999.
9. Pang, J., Seko, Y., Tokoro, T., Ichinose, S., Yamamoto, H. "Observation of ultrastructural changes in retinal pigment epithelium following exposure to blue light" *Graefe's Archive of Clinical and Experimental Ophthalmology*. 236:696-701, 1998.
10. Payne, D.J., Jost, T.R., Elliott, J.J., Eilert, B.G., Lott, L., Lott, K., Noojin, G.D., Hopkins, R.A. Jr., Lin, C.P., and Rockwell, B.A., "Cavitation thresholds in the rabbit retina pigmented epithelium," *Proceedings of SPIE*. 3601:27-31, 1999.
11. Wu, J., Gorman, A., Zhou, X., Sandra, C., Chen, E. "Involvement of Caspase-3 in Photoreceptor Cell Apoptosis Induced by In Vivo Blue Light Exposure" *Investigative Ophthalmology and Visual Science*. 43(10):3349-3354, 2002.
12. Wu, J., Chen, E., Soderberg, P.G. "Failure of ascorbic acid to protect against broadband blue light-induced retinal damage in rat" *Graefe's Archive of Clinical and Experimental Ophthalmology*. 237:855-860, 1999.
13. Finney, D. J. *Probit Analysis*. Cambridge University Press, New York, NY, ed. 3rd, 1971.
14. Cain, C.P. and Noojin, G.D. "A Comparison of Various Probit Methods for Analyzing Yes/No Data on a Log Scale." *AL/OE-TR-1996-0102*. Brooks AFB, TX, USAF Armstrong Laboratory: 46, 1996.
15. Thomas, R.J., Buffington, G.D., Irvin, L.J., *et al.* "Experimental and theoretical studies of broadband optical thermal damage to the retina." *Proceedings of SPIE*. 5688:411-422, 2005.
16. Thomas, R.J., Cain, C.P., Noojin, G.D., *et al.* "Extension of Thermal Damage Models of the Retina to Multi-Wavelength Sources." *Proceedings of ILSC*. 77-83, 2005.
17. Welch, A.J., Van Gemert, M. *Thermal Response of Tissue to Optical Radiation*. New York: Plenum Press; 1995.
18. Welch, A.J., Polhamus, G.D. "Measurement and prediction of thermal injury in the retina of the rhesus monkey." *IEEE Transactions in Biomedical Engineering*. BME-31:633, 2005.
19. Birngurber, R., Hillenkamp, F., Gabel, V-P. "Theoretical investigation of laser thermal retinal injury." *Health Physics*. 48:781-798, 1985.
20. Saraste, A., Pulkki, K. "Review: Morphologic and biochemical hallmarks of apoptosis" *Cardiovascular Research*. 45:528-537, 2000.
21. Zurgil, N., Shafran, Y., Fixler, D., Deutsch, M. "Analysis of Early Apoptotic Events in Individual Cells by Fluorescence Intensity and Polarization Measurements" *Biochemical and Biophysical Research Communications*. 290:1573-1582, 2002.
22. van Engeland, M., Ramaekers, F.C.S., Schutte, B., Reutelingsperger, C.P.M. "A Novel Assay to Measure Loss of Plasma Membrane Asymmetry During Apoptosis of Adherent Cells in Culture" *Cytometry*. 24:131-139, 1996.

23. Choucroun, P., Gillet, D., Dorange, G., Sawicki, B., Dewitte, J.D., "Comet assay and early apoptosis" *Mutation Research*. 478:89-96, 2001.
24. Andersson, M., Sjostrand, J., Petersen, A., Honarvar, A.K.S., Karlsson, J. "Caspase and Proteasome Activity during Staurosporin-Induced Apoptosis in Lens Epithelial Cells" *Investigative Ophthalmology and Visual Science*. 40(9):2623-2632, 2000.
25. Denton, M.L., Foltz, M.S., Estlack, L.E., Stolarski, D.J., Noojin, G.D., Thomas, R.J., Eikum, D., Rockwell, B.A. "Damage Thresholds for Exposure to NIR and Blue Lasers Using and *In-Vitro* RPE Cell System." *Investigative Ophthalmology and Visual Science*. Submitted.